ADVANCED FUNCTIONAL MATERIALS
www.afm-journal.de

Reversible Conversion between Schottky and Ohmic Contacts for Highly Sensitive, Multifunctional Biosensors

Luming Zhao, Hu Li, Jianping Meng, Aurelia Chi Wang, Puchuan Tan, Yang Zou, Zuqing Yuan, Junfeng Lu, Caofeng Pan, Yubo Fan, Yaming Zhang, Yan Zhang, Zhong Lin Wang,* and Zhou Li**

Schottky and Ohmic contacts–based electronics play an important role in highly sensitive detection of biomolecules and neural electric impulses, respectively. The reversible conversion between these two contacts appears especially important for multifunctional sensing by just one biosensor. Here, Schottky barrier height (SBH) is successfully tuned by triboelectric nanogenerator (TENG) and the same device is made to achieve reversible conversion between Schottky contact and Ohmic contact. In the same Schottky to Ohmic reversible (SOR) biosensor, highly sensitive detections of biomolecule (i.e., neurotransmitter) and neural electric signal are achieved at different contact states. The SOR biosensor reveals the feasibility of using one device to realize multifunctional detection. This work proposes a simple and significant method to achieve reversible tuning between the Schottky contact and Ohmic contact on one device by TENG, which exhibits great potential in developing multifunctional and high-sensitivity biosensors, rectifiers, and other functional electronic devices.

1. Introduction

In recent years, semiconductor nano/micro wire (NMW) based field effect transistors (FETs) are considered as good candidates for various kinds of sensing systems[1] because of their high surface to volume ratios.[2] When fabricating the NMW-based sensors, two types of metal-semiconductor contacts are usually formed between both ends of the NMW and metal electrodes, including Ohmic contact and Schottky contact.[3–6] For the Ohmic contact, it shows linear current-voltage characteristic at the contact region. Traditionally, to strengthen the sensitivity, Ohmic-contact based sensors were preferred to maximize the "gate-voltage" like effect by adsorbing molecules or bioelectricity.[7,8]

Recently, Schottky-contact devices have been demonstrated to show highly enhanced sensitivity to UV,[9] gas[10] and biomolecules.[3,8,11] Unlike Ohmic-contact based sensor, whose sensitivity depends strongly on the conductance change of NMWs, the sensing performance of the Schottky-contacted sensor is dominated by the Schottky barrier height (SBH).[4] The SBH at metal-semiconductor interface is very sensitive to the adsorbed charged/polar molecules that will change the SBH and affect the transport properties. The Schottky-contact devices become more and more important in biosensors,[12] rectifiers,[6] photodetectors,[13] and other applications.[14] Many innovative works have been made to tune the SBH, such as electron beam etching,[15] focused ion beam etching,[16] functioning the surface of zinc oxide (ZnO) by polymers[17] and piezotronic

L. M. Zhao, H. Li, Dr. J. P. Meng, P. C. Tan, Y. Zou, Dr. Z. Q. Yuan, Dr. J. F. Lu, Prof. C. F. Pan, Prof. Y. Zhang, Prof. Z. L. Wang, Prof. Z. Li
CAS Center for Excellence in Nanoscience
Beijing Key Laboratory of Micro-nano Energy and Sensor
Beijing Institute of Nanoenergy and Nanosystems
Chinese Academy of Sciences
Beijing 100083, China
E-mail: zhangyan@uestc.edu.cn; zhong.wang@mse.gatech.edu; zli@binn.cas.cn

L. M. Zhao, Dr. J. P. Meng, P. C. Tan, Y. Zou, Dr. Z. Q. Yuan, Dr. J. F. Lu, Prof. C. F. Pan, Prof. Z. L. Wang, Prof. Z. Li
School of Nanoscience and Technology
University of Chinese Academy of Sciences
Beijing 100049, China

The ORCID identification number(s) for the author(s) of this article can be found under https://doi.org/10.1002/adfm.201907999.

DOI: 10.1002/adfm.201907999

H. Li, Prof. Y. B. Fan
School of Biological Science and Medical Engineering
Beihang University
Beijing 100191, China

A. C. Wang, Prof. Z. L. Wang
School of Materials Science and Engineering
Georgia Institute of Technology
Atlanta, GA 30332, USA

Prof. C. F. Pan, Prof. Y. Zhang, Prof. Z. L. Wang, Prof. Z. Li
Center on Nanoenergy Research
School of Physical Science and Technology
Guangxi University
Nanning 530004, China

Y. M. Zhang, Prof. Y. Zhang
School of Physics
University of Electronic Science and Technology of China
Chengdu 610054, China

 © 2019 WILEY-VCH Verlag GmbH & Co. KGaA, Weinheim

effect.[18] The multifunctional application of biosensors based on only one nanowire device, which is realized by reversible conversion from Schottky contact to Ohmic contact, is still unreported yet.

The detections of neurotransmitter and nerve impulse between neuron synapses in situ are crucial for brain science[19] and clinical diagnosis.[20] These two detections of neurotransmitter and nerve impulse can be separately achieved by Schottky-contact biosensor and Ohmic-contact biosensor. If these two detections can be realized by just one tiny implantable device, it will be of great significance for clinical researchers and patients. In this study, the reversible conversion between Schottky contact and Ohmic contact was realized by the treatment of triboelectric nanogenerator (TENG) with high output voltage, it made the same one biosensor achieve high sensitive detection of neurotransmitter and neural electric impulse. The TENG can output high voltage,[21] which can lower the SBH effectively. After withdrawing the voltage impulse of TENG, the lowered SBH can recover gradually. By this tuning method, a Schottky to Ohmic reversible (SOR) biosensor was developed for achieving higher sensitive detections of DA in Schottky-contact state and neural electric signal in Ohmic-contact state. This study provides a new method to effectively tune SBH between metal and semiconductor and broadens the application scenarios of Schottky-contact devices. The as-fabricated multifunctional SOR biosensor verified the feasibility of using just one device to detect multiple information from biomolecules and bioelectric signals, and it could be developed to be small sized and implantable in the future.

2. Results and Discussion

2.1. Conception Diagram of Reversible Conversion between Schottky-Contact and Ohmic-Contact Biosensor

The neurotransmitter and nerve impulse detection between neuron synapses in situ will provide crucial information for brain science and nerve disease diagnosis. In this work, we proposed a method to conduct the conversion between Schottky contact to Ohmic contact, which provides the possibility to achieve high sensitive detection of neurotransmitter and nerve impulse just by one SOR biosensor (**Figure 1**). In the initial state, the Schottky contact is formed between metal and semiconductor NMW. A typical nonlinear nonsymmetrical *I–V* curve exhibits its rectification characteristic (Figure 1a). The high sensitive detection of low concentration of neurotransmitter can be achieved by using the Schottky-contact SOR biosensor (Figure 1a). After treated with high voltage pulse from TENG, the same one SOR biosensor can be converted to an Ohmic-contact device, which is greatly enhanced for bioelectrical signal recording (Figure 1b). After withdrawing the electric pulse from TENG, the Ohmic-contact biosensor can recover to the Schottky contact.

2.2. Tune SBH by TENG

To verify the tuning effect of TENG voltage on the SOR sensor, a rectified TENG is connected to the as-fabricated biosensor (**Figure 2**a). The optical image of the NMW-based biosensor

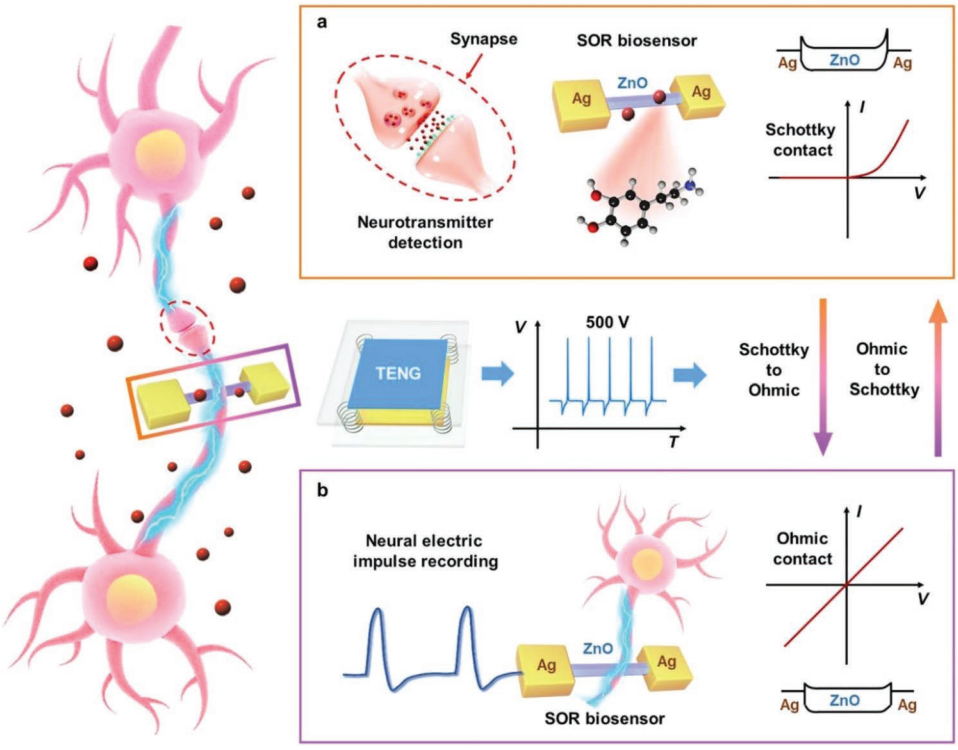

Figure 1. Conception diagram of Schottky to Ohmic reversible biosensor (SOR biosensor) for highly sensitive detection of neurotransmitter and neural electric impulse.

© 2019 WILEY-VCH Verlag GmbH & Co. KGaA, Weinheim

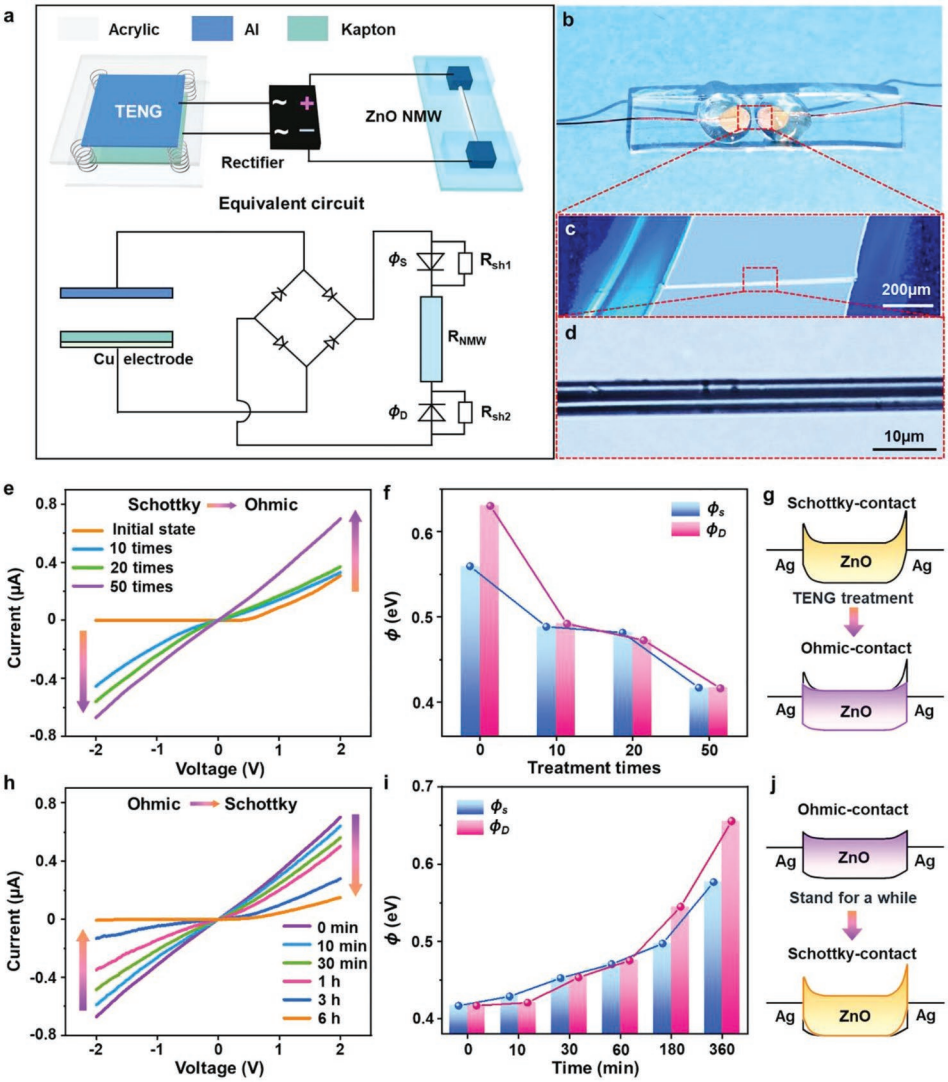

Figure 2. Devices, the equivalent circuit and the basic phenomenon of the SOR biosensor after different times of TENG treatment. a) Schematic diagram of the experiment setup and its equivalent circuit. b–d) Optical images of the SOR biosensor and ZnO NMW with different magnifications. e) *I–V* curves of the SOR biosensor after different times of TENG treatment. f) The SBHs of drain and source as a function of the TENG treatment times. g) The energy band diagram of the SOR biosensor before and after conversion from Schottky-contact to Ohmic-contact. h) *I–V* recovery curves of SOR biosensor from Ohmic-contact to Schottky-contact. i) The SBHs of drain and source as a function of the recovery time. j) The energy band diagrams of the ZnO NMW-based device after recovery from Ohmic-contact to Schottky-contact.

is shown in Figure 2b–d. The Ag paste electrodes at two ends were encapsulated with epoxy resin to protect them from oxidization in air and ensure the stable electric performance of the SOR sensor. The output voltages of TENG before and after rectified are about 500 and 350 V, respectively. (Figure S1a,b, Supporting Information). The TENG is periodically pressed by a motor at 1 Hz. Considering the inner resistance of TENG, the actual measured voltage on the biosensor is 20 V (Figure S1c, Supporting Information). The nonlinear and asymmetric *I–V* curve indicates that the as-fabricated biosensor formed Schottky contact with different SBHs on its ends (orange curve, Figure 2e).[22–24] The current of device increases with the treatment times. After treating the sensor for 50 times, the nonlinear *I–V* curve gradually turned to linear curve, (purple curve, Figure 2e) indicating that the rectification characteristic disappeared after the treatment. The calculated SBHs of drain and source were lowered from 0.63 and 0.57 to 0.416 eV (Figure 2f), respectively. The corresponding variation of energy band diagram is shown in Figure 2g. This result indicates that the SOR biosensor is converted from Schottky contact to Ohmic contact after TENG treatment. From the *I–V* curves in Ohmic contact state, the SBH lowing effect reached to saturation when the treatment times was more than 50. (Figure S2, Supporting Information).

During the recovery of the sensor, the periodical press of TENG was stopped. The linearity of *I–V* curve begins to change from 10 min and then recovers to nearly initial state gradually in 6 h (Figure 2h). The corresponding SBHs increase from 0.416 to 0.65 and 0.57 eV (Figure 2i), respectively. This result indicates that the converted Ohmic-contact (C-Ohmic-contact) can also recover to Schottky contact after withdrawing the electric pulse from TENG.

© 2019 WILEY-VCH Verlag GmbH & Co. KGaA, Weinheim

The SBH is recovered during this process (Figure 2j). It can be inferred from this phenomenon that the SBHs can also recover between the pressing cycles of TENG, the relationship between the cycle frequency and SBHs was investigated (Figure S3, Supporting Information). The larger the cycle frequency of TENG was applied, the smaller amount of SBH recovered during the pressing cycles of TENG, and thus the larger amount of SBH was lowered at the same TENG treatment times.

Figure 2 shows that the TENG treatment is an effective method to convert the SOR biosensor between Schottky contact and Ohmic contact. Besides the treatment times and cycle frequency, the TENG voltage will also affect the conversion (Figure S4, Supporting Information). The SBH modulation ability of TENG monotonously increases with the TENG voltage. At the same treatment times and frequency, the higher the TENG voltage was applied, the larger amount of SBH was lowered.

Besides in air, the TENG treatment is also effective in aqueous environment (Figure S5a–d, Supporting Information). The *I*–*V* curves of the encapsulated SOR biosensor also showed typical Schottky characteristics in water environment (Figure S5a, Supporting Information). After the TENG treatment, the SOR biosensor can also be converted from Schottky contact to Ohmic contact (Figure S5b, Supporting Information) and recover to Schottky contact after withdrawing the TENG (Figure S5c,d, Supporting Information).

Other semiconductor NMWs have also been treated by this method, including n-type GaN and p-type CuO. The similar phenomenon on GaN and opposite phenomenon on CuO were observed, which verified the universality of this TENG treatment method (Figure S6a,b, Supporting Information).

2.3. Mechanism Explanation of SBH Variation

According to previous studies,[24] strong electric field generated by high output voltage of TENG can drive the diffusion of oxygen vacancies in ZnO. Charges of oxygen vacancies at interface of metal-semiconductor (M-S) contact can effectively control SBH.

In previous researches,[24,25] the driving and generating processes of oxygen vacancies have been well studied. The oxygen vacancies are driven to move along its *c*-axis direction as interstitial ions owing to the generated unidirectional pyroelectric field of devices. Thus, we use the classical model to show the physical process of oxygen vacancies being driven to accumulate at the contact when the devices are treated by TENG.

The *I*–*V* properties of metal-semiconductor-metal (M-S-M) junction are obviously different due to different contact behaviors in different physical conditions,[23,24] and there were greatly different experimental *I*–*V* characteristics for different M-S-M contact behaviors. In addition, previous research has demonstrated the SBH both decreased in two ends of M-S-M junction when the device is treated by macroscopic electric field.[26] For simplification, we choose an ideal classic M-S-M model (one end is perfect contact), and the electric property is determined mainly by the forward voltage.[23] In this study, this simplified model is used to demonstrate the variety of one interface characteristic when the devices is treated by TENG. The physical process of conversion from Schottky to Ohmic contact is shown in **Figure 3**.

In the initial state, Ag paste and one end of n-type ZnO NMW formed Schottky contact, a Schottky barrier is created at the interface, the schematic atomic structure and energy-band diagram of the interface is shown in Figure 3a. In the

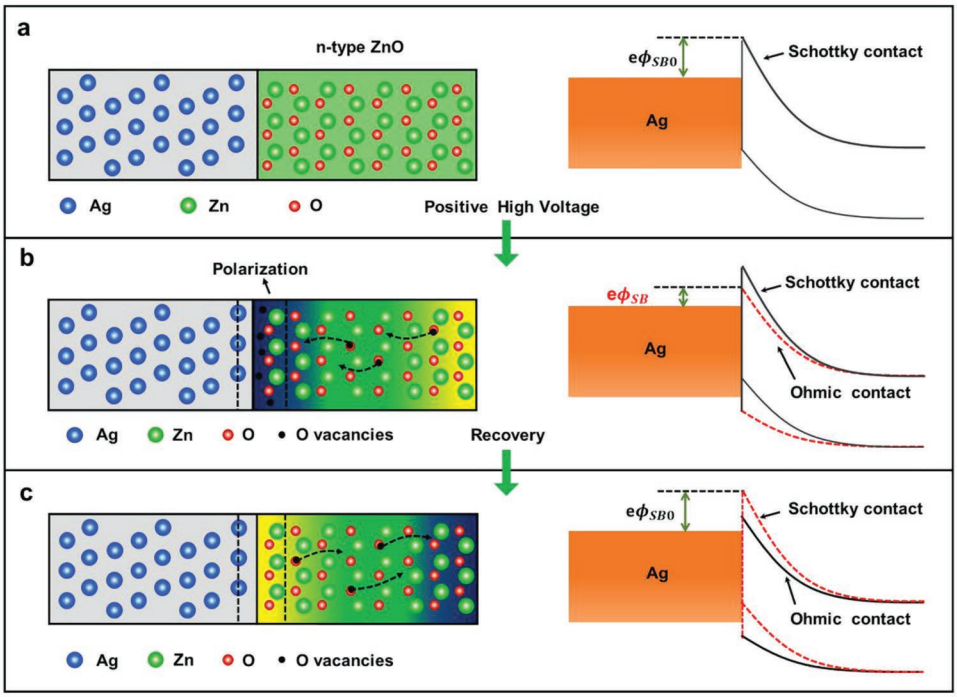

Figure 3. Polarization model and schematic diagram of SBH variation. a) The model of an M-S contact consisted of Ag and n-type ZnO and the initial state is Schottky contact. b) The oxygen vacancies are driven by positive high voltage of TENG, and the positive charges are accumulated at contact, then the Schottky contact can be convert to Ohmic contact. c) The oxygen vacancies diffuse slowly at opposite direction after withdrawing the treatment of positive high voltage of TENG, and the positive charges vanish and Schottky barrier arise.

© 2019 WILEY-VCH Verlag GmbH & Co. KGaA, Weinheim

case of Schottky to Ohmic contact, the transport characteristics will show the switch when positive charges accumulate at contact interface, as shown in Figure 3b. In the case of Ohmic to Schottky contact, after withdrawing the treatment of TENG, oxygen vacancies diffuse at opposite direction. Compared with the Schottky to Ohmic conversion process, the Ohmic to Schottky conversion process is significantly slower. As a result, positive charges disappear slowly, and Schottky barrier arises after a long time. The contact converted from Ohmic to Schottky is shown in Figure 3c.

For a one-dimensional model, the built-in potential φ_{bi} is given by[27–29]

$$\varphi_{bi} = \frac{q}{2\varepsilon_s}\left(N_A W_{Dp}^2 + \rho_{polar} W_{polar}^2 + N_D W_{Dn}^2\right) \quad (1)$$

In this equation, the N_D and N_A are the donor and acceptor concentration, severally. Additionally, the ρ_{polar} and W_{polar} are the polarization charges density and the distribution width of oxygen vacancies, respectively, which are functions of time that are gradually built up as the TENG bias is applied. The W_{Dp} and W_{Dn} are the widths of depletion region on the p-type and n-type, respectively. Because the ZnO NMW used in this work is n-type, the N_A and W_{Dp} can be assumed to be zero in this study. Current-voltage characteristics of the M-S junction is given by[29]

$$J = J_0 exp\left(\frac{q^2 \rho_{polar} W_{polar}^2}{2\varepsilon_s kT}\right)\left[exp\left(\frac{qV}{kT}\right) - 1\right] \quad (2)$$

where the V is the bias voltage, k_B and T are the Boltzmann constant and temperature, respectively, J_0 is the saturation current density, ε_s is the permittivity of the material. For M-S contact, J_0 is given by[29]

$$J_0 = \frac{q^2 D_n N_c}{kT}\sqrt{\frac{2qN_D(\varphi_{bi0} - V)}{\varepsilon_s}} exp\left(-\frac{q\Phi_{SB0}}{kT}\right) \quad (3)$$

where the N_c and D_n are the effective density of states at conduction band and electron diffusion coefficients, respectively, Φ_{SB0} and φ_{bi0} are SBH and built-in potential without polarization charges. Many previous work have investigated the influence about polarization charges to SBH.[27,28] Thus, after polarization, the initial SBH (Φ_{SB0}) of one dimensional M-S model can be decreased to Φ_{SB}[29]

$$\Phi_{SB} = \Phi_{SB0} - \frac{q\rho_{polar} W_{polar}^2}{2\varepsilon_s} \quad (4)$$

2.4. Multifunctional SOR Biosensor at Schottky-Contact State for DA Detection

It has been reported that Schottky-contact biosensor has enhanced sensitivity for molecule detection compared with Ohmic-contact biosensor.[3,12] In this work, the SOR biosensors with Schottky-contact mode and Ohmic-contact mode were used to detect dopamine (DA) (**Figure 4**a), whose level is an important indicator to the diagnosis of Alzheimer's[30] and Parkinson's diseases.[31] The current of *I–V* curve for the Schottky-contact biosensor at the positive voltage decreases obviously as the DA hydrochloride concentration increases (Figure 4b). *I–t* curve confirms this result further (Figure 4d). The calculated SBH according to the *I–V* curve ranged from 0 to 2 V increases as the DA hydrochloride concentration increases (Figure S7, Supporting Information). This is because that the negatively charged DA molecules adsorbed on the ZnO surface will deplete the electrons in ZnO NMW. This is equivalent to a negative potential gating that results in a decreased electron density of the SOR biosensor. Such a negative "gate" acts the same by increasing the conduction and valence bands of ZnO simultaneously and raising the SBH, thus decreasing the output current (Figure 4c).[12] As the DA molecules desorb from ZnO surface in PBS, the response current gradually recovered (Figure S8, Supporting Information), the falling time and recovery time are 15 and 25 s, respectively.

Unlike Schottky-contact biosensor, molecule adsorption on the surface of Ohmic-contact biosensor affects the resistance of the ZnO NMW; the linear *I–V* curves before and after DA molecule detection are almost unchanged (Figure 4f). *I–t* curve barely changed (Figure 4e). It is insensitive to the low concentration of DA. The absolute and relative current response ($\Delta I/I_0$) of the Schottky-contact biosensor is ten times that of the Ohmic-contact biosensor at 10 µmol mL^{-1} (Figure 4g). Additionally, the C-Ohmic-contact biosensor is also insensitive to the low concentration of DA (Figure S9, Supporting Information). A sensitivity of 0.1 µmol mL^{-1} for DA detection was obtained from the Schottky-contact biosensor (Figure 4d), and in the case of the SOR biosensor in Ohmic-contact state, it is almost insensitive for DA ranging from 0.01 to 10 µmol mL^{-1}. The Schottky-contact sensor shows enhanced sensitivity because the adsorption of DA molecules basically changes the SBH at local Ag–ZnO interface rather than the conductance of ZnO NMW. At the fixed basing voltage, the current of the sensor has exponential relation with SBH.[6] Therefore, the same amount of adsorbed charged biomolecules can definitely lead to more sensitive responses of output signals in Schottky-contacted sensors which makes it has higher sensitivity for the molecule detection at low concentration compared with Ohmic-contact biosensor.[11]

2.5. Multifunctional SOR Biosensor in Ohmic-Contact State for Recording Neural Electric Impulse

It is known that by the release of neurotransmitters, nerve impulse can be transmitted across synapses between neurons and conducted along the nervous fibers in the form of electrical signals.[32] We then used the same SOR biosensor to detect the neural electric impulse of the bullfrog sciatic nerve trunk before and after conversion (**Figure 5**a,b). All the animal experiments were performed strictly in accordance with the "Beijing Administration Rule of Laboratory Animals" and the national standard "Laboratory Animal Requirements of Environment and Housing Facilities" (GB 14925-2001). The primary and enlarged output current responses of the SOR biosensors with Schottky-contact and C-Ohmic-contact to electrostimulation are systematically summarized in Figure 5c,d under different stimulation voltages. When the amplitude of the voltage pulse is lower than 0.2 V, the intensity of the electrostimulation do not reach the

© 2019 WILEY-VCH Verlag GmbH & Co. KGaA, Weinheim

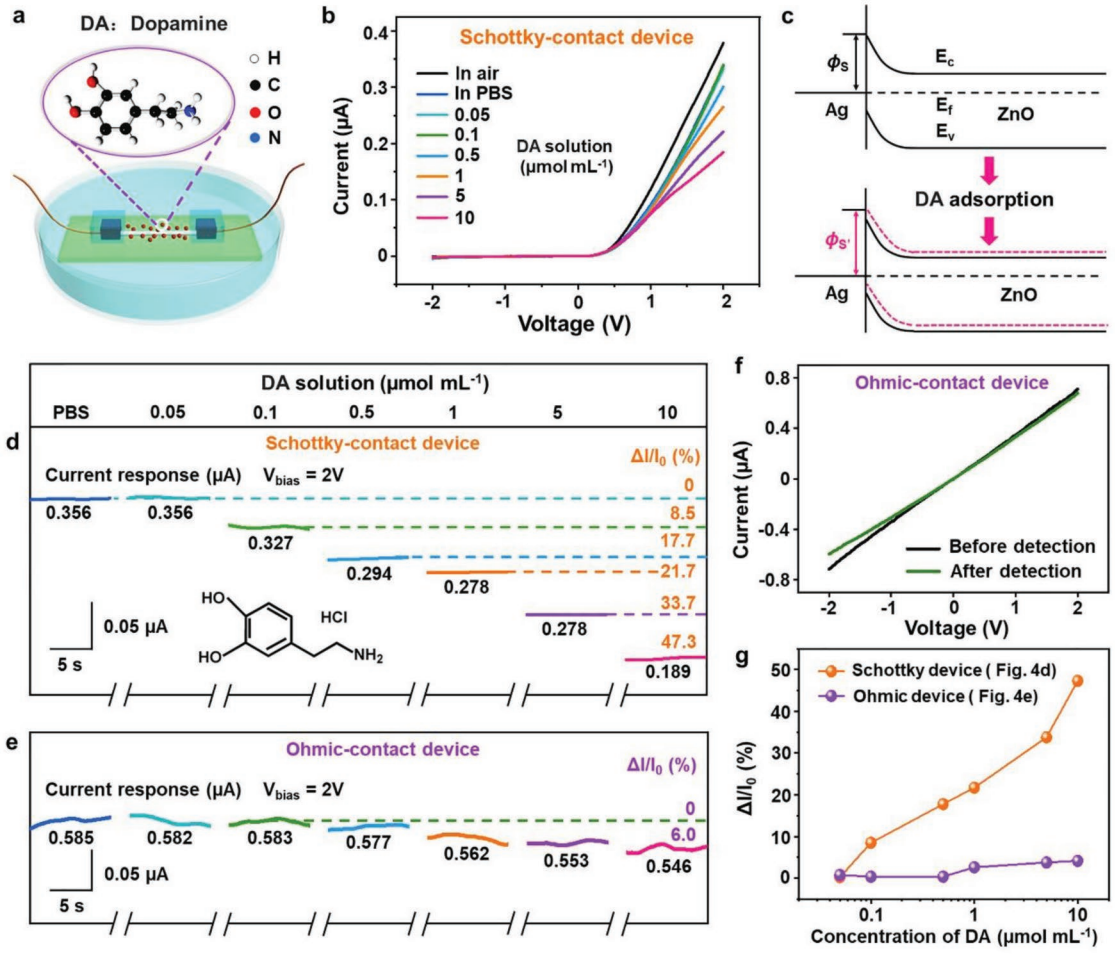

Figure 4. The Schottky-contact with much higher sensitivity for low concentrated dopamine (DA) detection compared with Ohmic-contact. a) The schematic diagram of DA detection process by biosensor. b) *I–V* curves of a Schottky-contact biosensor in different concentrations of DA hydrochloride. c) Energy band diagram of the ZnO in DA hydrochloride solution. d) *I–t* curves of a Schottky-contact biosensor in different concentrations of DA hydrochloride. e) *I–t* curves of an Ohmic-contact biosensor in different concentrations of DA hydrochloride. f) *I–V* curves of the Ohmic-contact SOR biosensor before and after dopamine hydrochloride detection. g) Absolute and relative current response of Schottky-contact and Ohmic-contact biosensor in (d) and in (e) with different concentrations of DA hydrochloride.

threshold value (i.e., 0.2 V) of the nerve fiber. Therefore, there is no vibrant contraction of the frog's gastrocnemius muscle is observed and no action potential is recorded by SOR biosensor in Schottky-contact state or C-Ohmic-contact state.

The feature signal of action potential is observed in C-Ohmic-contact state once the stimulating voltage reaches to 0.2 V (Figure 5d). The corresponding amplitude of feature signal is ranged from 0.5 to 7 nA. Whereas, the weak feature signal of action potential is not detected until the simulating voltage reaches up to 0.6 V (Figure 5c) in Schottky-contact state. The corresponding amplitude of feature signal is about 0.1 nA. The signal recorded by the SOR biosensor in C-Ohmic-contact exhibited a wider range and higher intensity comparing with the SOR biosensor in Schottky contact (Figure 5e). Compared with the Schottky contact, the signal intensity of action potential recorded by the SOR biosensor in C-Ohmic-contact state is enhanced by dozens of times (Figure 5f).

This method of recording neural electric impulse has been reported in previous literatures.[31] When the action potential in the bullfrog sciatic nerve flows passes the n-type ZnO NMW, it is similar to a gate voltage (V_G) applying on the device.[33] The positive V_G increases electron concentration to make the conduction band bent towards the Fermi level. Therefore, the conduction of the ZnO NMW became higher. Similarly, the negative V_G decreases electron concentration, which will make the conduction band bent away from the Fermi level. The conduction of the ZnO NMW decreased.[32,34,35] The sensitivity of the ZnO NMW sensor, or its ability to receive and amplify the V_G, is usually defined as transconductance.[32,36] The relationship between the extrinsic transconductance (g_{ex}) measured in experiments and the intrinsic transconductance (g_{in}) is[35,37]

$$g_{ex} = \frac{g_{in}}{1 + g_{in}R_S + (R_S + R_D)/R_{wire}} \quad (5)$$

where, R_S and R_D represent the contact resistance of source and drain, respectively. R_{wire} represents the resistance of the

© 2019 WILEY-VCH Verlag GmbH & Co. KGaA, Weinheim

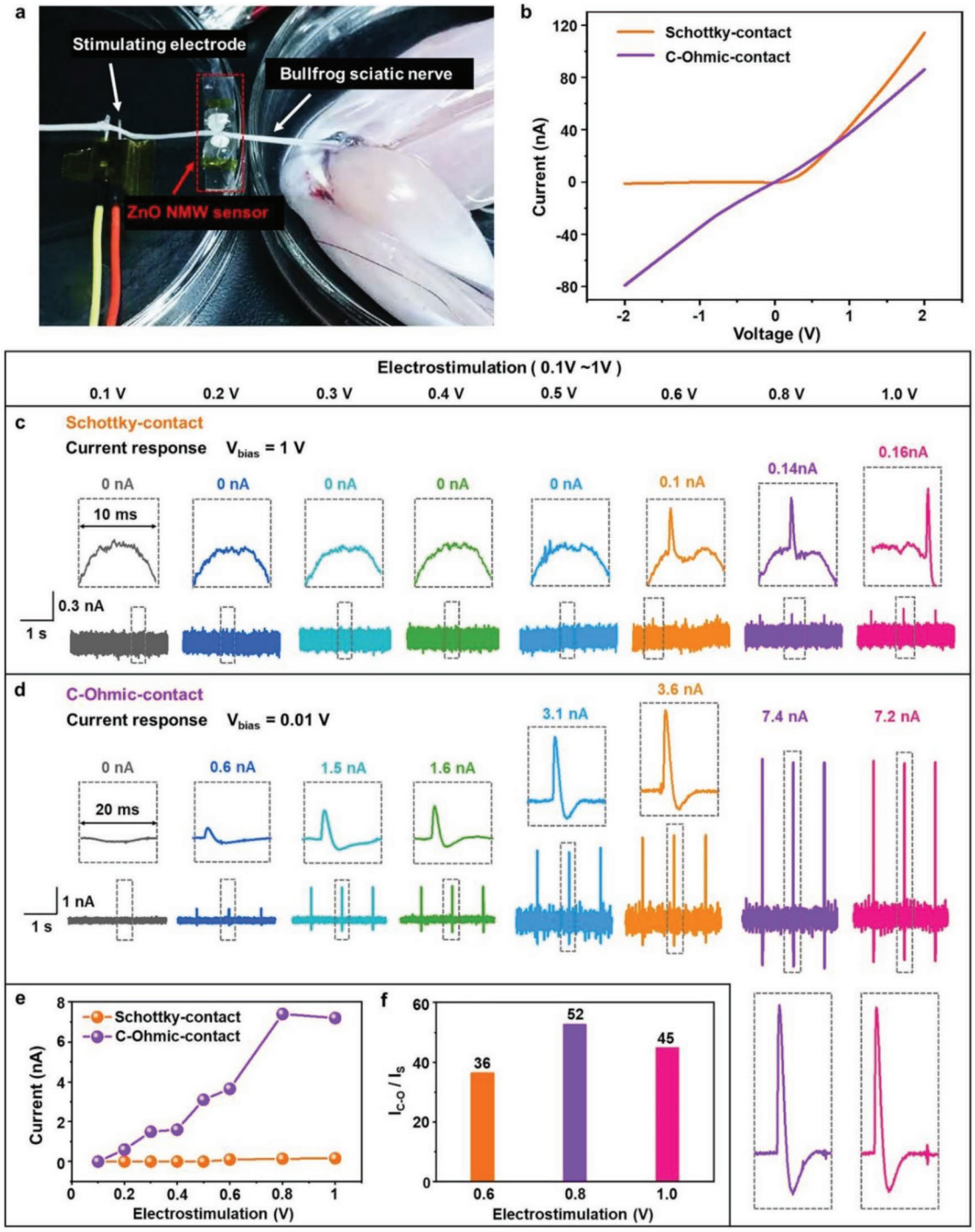

Figure 5. Enhanced neural electric impulse detection by converted Ohmic-contact ZnO NMW-based device. a) Experimental setup of the sciatic nerve signal detection by ZnO NMW-based device. b) *I–V* curves of the ZnO NMW-based device before and after the conversion from Schottky-contact (orange) and C-Ohmic-contact (purple). c,d) The resulting neural electrical responses measured with Schottky-contact and C-Ohmic-contact sensors after stimulated with different voltage pulses from 0.1 to 1 V. e) Plot of current spike amplitude as a function of electrostimulation, where signals were recorded by Schottky-contact (orange) and C-Ohmic-contact sensors (purple), respectively. f) Enhancement of neural electric impulse detection by the same ZnO NMW-based sensor in C-Ohmic-contact and Schottky-contact under different electrostimulation (0.6, 0.8, and 1.0 V).

ZnO NW. Compared with the Schottky mode, C-Ohmic mode has lower source and drain contact resistance (R_S and R_D), which makes the C-Ohmic-contact SOR biosensor has the advantage of higher sensitivity (extrinsic transconductance, g_{ex}) for recording neural electric impulse (Figure S10, Supporting Information). As shown in Figure 5c,d, the SOR the sensitivity

© 2019 WILEY-VCH Verlag GmbH & Co. KGaA, Weinheim

of the SOR biosensors in Schottky-contact state is 0.16 nS (0.16 nA/1 V), and the sensitivity of the SOR biosensors in Ohmic-contact state is 720 nS (7.20 nA/0.01 V). This phenomenon was in accordance with the transconductance modulation mechanism.

2.6. Multifunctional Demonstration of SOR Biosensor in Different Contact States

In order to achieve the objectives of concept in Figure 1, we carried out the DA detection and neural electric impulse recording using the same one SOR biosensor before and after TENG treatment to confirm the simultaneous sensitive detection of neurotransmitter and neural electric impulse (**Figure 6**a). A constant voltage was applied on the two ends of SOR sensor by an electrometer (KEITHLEY 6517B). The stimulation on neurons (nerve fiber) was applied by signal generator (ArbStudio 1104). The two electrodes of the signal generator were posited under the nerve fiber on one side of the sensor.

In the initial state, the SOR biosensor in Schottky-contact state shows high sensitivity to DA molecules, (Figure 6b,c). In the case of recording neural electric impulse evoked by the electrostimulation (1 V, 1 Hz, 0.1 ms) (Figure 6e), the current spikes measured by the Schottky-contact SOR biosensor at the fixed bias voltage of 1 V is weak, the spike amplitude is only about 0.206 nA (Figure 6f). After converting the Schottky-contact SOR biosensor to Ohmic-contact SOR biosensor by TENG treatment (Figure 6d), the current spike amplitude recorded by the SOR biosensor in C-Ohmic-contact under 0.01 V increased to 3.3 nA (Figure 6g), which is about 16 times greater than that recorded by the same one SOR biosensor in Schottky-contact state (Figure 6h). Moreover, the sensitivity (g_{ex}) of the SOR biosensors towards neural electric impulse were significantly enhanced after conversion (0.206 nS at Schottky contact and 325 nS at C-Ohmic contact). The C-Ohmic-contact SOR

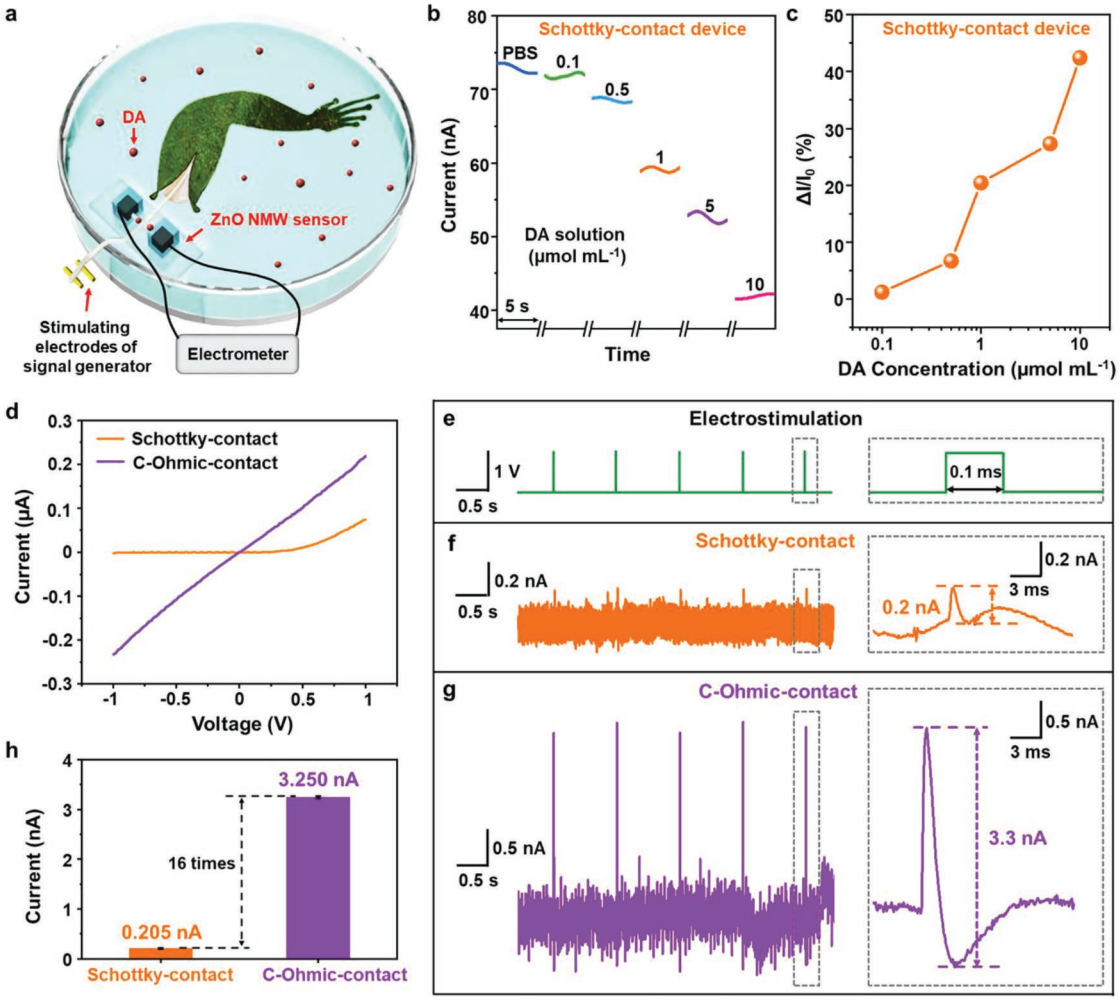

Figure 6. Neurotransmitter detection by SOR biosensor in Schottky-contact and neural electric impulse detection by SOR biosensor in C-Ohmic-contact by a SOR biosensor. a) Schematic diagram of SOR biosensor for sensitive detection of DA molecule and neural electric impulse recording. b,c) *I–t* curves and the absolute and relative current response of a Schottky-contact SOR biosensor with different DA hydrochloride concentrations. d) *I–V* curves of the SOR biosensor before and after conversion between Schottky-contact (orange) and C-Ohmic-contact (purple). e) The trace of nerve fiber electrostimulation with voltage pulses (1 V, 1 Hz, 0.1 ms). f,g) The resultant electrical responses measured with SOR biosensor in Schottky-contact state and C-Ohmic-contact state, respectively. h) Comparison of average current spike amplitudes in (f) and (g).

© 2019 WILEY-VCH Verlag GmbH & Co. KGaA, Weinheim

biosensor has weak response to the DA molecules (Figure S9, Supporting Information). Based on above results, by using a high voltage TENG to tune the SBH, we can convert a biosensor between Schottky contact and Ohmic contact for realizing a high sensitive detection of two distinctive signals from neurotransmitter and neural electric impulse by one biosensor, which is based on a single ZnO NMW device.

3. Conclusion

We have proposed a method to achieve the reversible conversion between Schottky contact and Ohmic contact by TENG treatment effectively. The conception is that the SBH of the device decreases with the TENG treatment and will gradually recover with time after withdrawing the TENG treatment. The conversion can be attributed to the diffusion of oxygen vacancies in ZnO NMW as driven by TENG voltage pulses. By this method, a SOR biosensor can have different advantages under different states. In this paper, the same one SOR biosensor in Schottky contact state achieves the high sensitive detection of the low concentration of dopamine (0.1 μmol mL^{-1}). After converting to Ohmic contact, an enhanced sensitivity to the neural electric impulse is realized by the same one SOR biosensor. Our demonstration for a comprehensive multifunctional sensor is important for detecting neurotransmitter and nervous impulse in physiological environment, which is crucial for brain science and clinical diagnosis. This work also presents a universal approach of tuning SBH reversibly, which will broaden the function of Schottky-contact device and provide a promising way to improve the performance of various sensing systems, rectifiers, photodetectors and other related electronics.

4. Experimental Section

Synthesis of ZnO NMWs and Fabrication of SOR Biosensor: The ZnO NMWs were synthesized by gas-solid (V-S) method as follows: 1) A silicon wafer was cut in the size of 1 cm × 1 cm, and then ultrasonically washed with acetone, ethanol and deionized water, respectively. Finally, the samples were dried with nitrogen gas as the growth substrates for ZnO NMWs. 2) 1 g of ZnO powder (purity, 99.99%) and 1 g of carbon powder (purity, 99.99%) were mixed and ground hook. 3) The quartz boat with mixed powder was placed in a quartz tube. The silicon substrate was placed horizontally on top of the quartz boat. Argon gas and oxygen gas ($Ar:O_2 = 10:1$) were introduced, and the quartz tube was heated to 1050 °C for 40 min to obtain ZnO NMWs.

The SOR biosensor was fabricated by laying an individual ZnO NMW onto the center of the glass substrate. Both ends of the nano/microwire were fixed on the substrate by silver paste. A thin epoxy layer was covered on the sliver paste to form the water-proof layer.

Fabrication of TENG: Aluminum (Al) foils and Kapton films were prepared with the same size (8 cm × 8 cm × 100 μm). The Al foils and Kapton films were cleaned with alcohol. Copper (Cu) film (50 nm) was deposited on the surface of Kapton film as the back electrode by magnetron sputtering. Both Al foil and Kapton film were polished in the same direction for 2 times using sandpapers with a grit size of 3000 #. Al foil was applied as both tribo-layer and electrode. Al electrode and Cu electrode were connected with copper wire by silver (Ag) paste. To ensure the stability of the electrode of TENG, the Ag paste was covered by a layer of kapton tape. The Ag paste was enfolded by the back Cu electrode and bond layer to avoid the oxidation of Ag paste and Cu. Both tribo-layers were fixed on the two acrylic plates (10 cm × 10 cm × 500 mm). Spacer was made of springs, keeping the Kapton film at a fixed distance away from the Al foil.

Device and Performance Characterization: Morphology of the SOR biosensors was characterized using an optical microscope (Nikon ECLIPSE 3 × 2 STAGE JAPAN). The output voltage of TENG was measured by digital phosphor oscilloscope (Tektronix DPO 3034). The *I–V* curves of the SOR biosensor were measured by semiconductor characterization system (Keithley 4200A-SCS).

Detection of DA Molecules and Recording of Neural Electric Impulses: During the detection of DA, *I–t* curves were recorded at a bias voltage of 2 V by electrometer (KEITHLEY 6517B). The bullfrog sciatic nerve trunk was immersed into the Ringer's solution for 10 min to keep activity after preparation. Then, the bullfrog sciatic nerve trunk was placed aligned across the SOR biosensor and stimulated by the electrodes connected to the signal generator (ArbStudio 1104). The electrostimulation was the voltage pulses with amplitude ranging from 0.1 to 1 V and frequency of 1 Hz, and the effective time of every pulse was 0.1 ms. The *I–t* curves of the SOR biosensor were continuously recorded at a fixed voltage by electrometer (KEITHLEY 6517B). Throughout the experiment, the bullfrog sciatic nerve trunk was kept wet by Ringer's solution.

Supporting Information

Supporting Information is available from the Wiley Online Library or from the author.

Acknowledgements

The authors thank the support of National Key R&D Project from Minister of Science and Technology, China (2016YFA0202703), National Natural Science Foundation of China (Nos. 61875015, 31571006, 81601629, and 21801019), the Beijing Natural Science Foundation (2182091), China Postdoctoral Science Foundation (2018M641148), Beijing Council of Science and Technology (Z181100004418004), and the National Youth Talent Support Program.

Conflict of Interest

The authors declare no conflict of interest.

Author Contributions

L.M.Z., H.L., J.M., and A.C.W. contributed equally to this work. Z.L., L.M.Z. and H.L. conceived the idea and designed the experiment. Z.L., Z.L.W., and Y.Z. guided the project. L.M.Z. and H.L. fabricated the devices and performed the experiment. L.M.Z., H.L., J.M., A.C.W., and Z.L. analyzed the data. Z.Q.Y., J.L., and C.P. offered the ZnO micro/nanowires. L.M.Z., H.L., Y.Z., and P.T. performed the animal experiment. Y.Z., J.M., L.M.Z., Y.M.Z., and H.L. developed the theoretical models. L.M.Z., H.L., J.M., and A.C.W. drew the figures. L.M.Z., H.L., J.M., and A.C.W. prepared the manuscript. All authors discussed and reviewed the manuscript.

Keywords

multifunctional biosensors, reversible conversion, Schottky/Ohmic contacts, semiconductor nanowires, triboelectric nanogenerators

Received: September 26, 2019
Revised: October 19, 2019
Published online:

© 2019 WILEY-VCH Verlag GmbH & Co. KGaA, Weinheim

[1] a) Y. Cui, Q. Wei, H. Park, C. M. Lieber, *Science* **2001**, *293*, 1289; b) A. Menzel, K. Subannajui, F. Güder, D. Moser, O. Paul, M. Zacharias, *Adv. Funct. Mater.* **2011**, *21*, 4342.
[2] a) F. Patolsky, B. P. Timko, G. H. Yu, Y. Fang, A. B. Greytak, G. F. Zheng, C. M. Lieber, *Science* **2006**, *313*, 1100; b) T. Shaymurat, Q. Tang, Y. Tong, L. Dong, Y. Liu, *Adv. Mater.* **2013**, *25*, 2269; c) Z. T. Lin, Y. Li, J. Gu, H. Wang, Z. Zhu, X. Hong, Z. Zhang, Q. Lu, J. Qiu, X. Wang, J. Bao, T. Wu, *Adv. Funct. Mater.* **2018**, *28*, 1802482.
[3] P. H. Yeh, Z. Li, Z. L. Wang, *Adv. Mater.* **2009**, *21*, 4975.
[4] Y. Hu, J. Zhou, P. H. Yeh, Z. Li, T. Y. Wei, Z. L. Wang, *Adv. Mater.* **2010**, *22*, 3327.
[5] E. H. Rhoderick, R. H. Williams, *Metal-Semiconductor Contacts*, 2nd ed., Clarendon Press, Oxford **1988**.
[6] S. M. Sze, K. K. Ng, *Physics of Semiconductor Devices*, John wiley & sons, **2006**.
[7] T.-S. Pui, A. Agarwal, F. Ye, N. Balasubramanian, P. Chen, *Small* **2009**, *5*, 208.
[8] R. Yu, C. Pan, J. Chen, G. Zhu, Z. L. Wang, *Adv. Funct. Mater.* **2013**, *23*, 5868.
[9] J. Zhou, Y. Gu, Y. Hu, W. Mai, P.-H. Yeh, G. Bao, A. K. Sood, D. L. Polla, Z. L. Wang, *Appl. Phys. Lett.* **2009**, *94*, R33.
[10] a) T. Y. Wei, P. H. Yeh, S. Y. Lu, Z. L. Wang, *J. Am. Chem. Soc.* **2009**, *131*, 17690; b) R. Zhou, G. Hu, R. Yu, C. Pan, Z. L. Wang, *Nano Energy* **2015**, *12*, 588.
[11] R. Yu, S. Niu, C. Pan, Z. L. Wang, *Nano Energy* **2015**, *14*, 312.
[12] R. Yu, C. Pan, Z. L. Wang, *Energy Environ. Sci.* **2013**, *6*, 494.
[13] a) S. Liu, Q. Liao, S. Lu, Z. Zhang, G. Zhang, Y. Zhang, *Adv. Funct. Mater.* **2016**, *26*, 1347; b) J. Guo, Y. Liu, Y. Ma, E. Zhu, S. Lee, Z. Lu, Z. Zhao, C. Xu, S.-J. Lee, H. Wu, K. Kovnir, Y. Huang, X. Duan, *Adv. Mater.* **2018**, *30*, 1705934; c) W. Ouyang, F. Teng, J.-H. He, X. Fang, *Adv. Funct. Mater.* **2019**, *29*, 1807672.
[14] a) J. H. Song, Y. Zhang, C. Xu, W. Z. Wu, Z. L. Wang, *Nano Lett.* **2011**, *11*, 2829; b) J. Zhang, A. Yang, X. Wu, J. van de Groep, P. Tang, S. Li, B. Liu, F. Shi, J. Wan, Q. Li, Y. Sun, Z. Lu, X. Zheng, G. Zhou, C.-L. Wu, S.-C. Zhang, M. L. Brongersma, J. Li, Y. Cui, *Nat. Commun.* **2018**, *9*, 5289; c) P. H. Rekemeyer, S. Chang, C.-H. M. Chuang, G. W. Hwang, M. G. Bawendi, S. Gradecak, *Adv. Energy Mater.* **2016**, *6*, 1600848.
[15] L. M. Moretto, M. Tormen, M. De Leo, A. Carpentiero, P. Ugo, *Nanotechnology* **2011**, *22*, 185305.
[16] G. Han, D. Weber, F. Neubrech, I. Yamada, M. Mitome, Y. Bando, A. Pucci, T. Nagao, *Nanotechnology* **2011**, *22*, 275202.
[17] C. Lao, Y. Li, C. P. Wong, Z. L. Wang, *Nano Lett.* **2007**, *7*, 1323.
[18] a) J. Zhou, P. Fei, Y. Gu, W. Mai, Y. Gao, R. Yang, G. Bao, Z. L. Wang, *Nano Lett.* **2008**, *8*, 3973; b) X. Wang, J. Song, J. Liu, Z. L. Wang, *Science* **2007**, *316*, 102; c) W. Wu, Y. Wei, Z. L. Wang, *Adv. Mater.* **2010**, *22*, 4711; d) K. Jenkins, V. Nguyen, R. Zhu, R. Yang, *Sensors* **2015**, *15*, 22914; e) H. Yuan, T. Lei, Y. Qin, R. Yang, *Nano Energy* **2019**, *59*, 84; f) R. Zhu, R. Yang, *Nanotechnology* **2014**, *25*, 345702.
[19] a) D. S. Bassett, O. Sporns, *Nat. Neurosci.* **2017**, *20*, 353; b) G. Hong, C. M. Lieber, *Nat. Rev. Neurosci.* **2019**, *20*, 330.
[20] B. Xu, M. Zhu, W. Zhang, X. Zhen, Z. Pei, Q. Xue, C. Zhi, P. Shi, *Adv. Mater.* **2016**, *28*, 3411.
[21] a) F. R. Fan, Z. Q. Tian, Z. L. Wang, *Nano Energy* **2012**, *1*, 328; b) Z. L. Wang, *ACS Nano* **2013**, *7*, 9533; c) H. Li, C. Zhao, X. Wang, J. Meng, Y. Zou, S. Noreen, L. Zhao, Z. Liu, H. Ouyang, P. Tan, M. Yu, Y. Fan, Z. L. Wang, Z. Li, *Adv. Sci.* **2019**, *6*, 1801625; d) L. Zhao, Q. Zheng, H. Ouyang, H. Li, L. Yan, B. Shi, Z. Li, *Nano Energy* **2016**, *28*, 172.
[22] L. J. Brillson, Y. Lu, *J. Appl. Phys.* **2011**. *109*, 121301.
[23] Z. Zhang, K. Yao, Y. Liu, C. Jin, X. Liang, Q. Chen, L. M. Peng, *Adv. Funct. Mater.* **2007**, *17*, 2478.
[24] a) Z. Zhang, C. Jin, X. Liang, Q. Chen, L.-M. Peng, *Appl. Phys. Lett.* **2006**, *88*, 073102; b) Y. Ding, Y. Liu, S. Niu, W. Wu, Z. L. Wang, *J. Appl. Phys.* **2014**, *116*, 154304.
[25] S. J. Skinner, J. A. Kilner, *Mater. Today* **2003**, *6*, 30.
[26] F. Xue, L. Zhang, X. Feng, G. Hu, F. R. Fan, X. Wen, L. Zheng, Z. L. Wang, *Nano Res.* **2015**, *8*, 2390.
[27] Y. Zhang, Y. Liu, Z. L. Wang, *Adv. Mater.* **2011**, *23*, 3004.
[28] Y. Zhang, Y. Leng, M. Willatzen, B. Huang, *MRS Bull.* **2018**, *43*, 928.
[29] C. Pan, J. Zhai, Z. L. Wang, *Chem. Rev.* **2019**, *119*, 9303.
[30] M. A. Piggott, E. F. Marshall, N. Thomas, S. Lloyd, J. A. Court, E. Jaros, D. Burn, M. Johnson, R. H. Perry, I. G. McKeith, C. Ballard, E. K. Perry, *Brain* **1999**, *122*, 1449.
[31] J. Lotharius, P. Brundin, *Nat. Rev. Neurosci.* **2002**, *3*, 932.
[32] B. Tian, C. M. Lieber, *Annu. Rev. Anal. Chem.* **2013**, *6*, 31.
[33] G. Buzsáki, C. A. Anastassiou, C. Koch, *Nat. Rev. Neurosci.* **2012**, *13*, 407.
[34] S. J. Tans, A. R. M. Verschueren, C. Dekker, *Nature* **1998**, *393*, 49.
[35] G. Zheng, W. Lu, S. Jin, C. M. Lieber, *Adv. Mater.* **2004**, *16*, 1890.
[36] C. K. Tzahi, B. P. Timko, L. E. Weiss, C. M. Lieber, *Proc. Natl. Acad. Sci. USA* **2009**, *106*, 7309.
[37] A. Zhang, C. M. Lieber, *Chem. Rev.* **2016**, *116*, 215.

© 2019 WILEY-VCH Verlag GmbH & Co. KGaA, Weinheim